The American Journal of Pathology, Vol. 181, No. 1, July 2012

http://dx.doi.org/10.1016/j.ajpath.2012.03.013

Short Communication

Quantitative Proteomics Reveals that miR-155 Regulates the PI3K-AKT Pathway in Diffuse Large B-Cell Lymphoma

Xin Huang,*† Yulei Shen,* Miao Liu,* Chengfeng Bi,* Chunsun Jiang,* Javeed Iqbal,* Timothy W. McKeithan,* Wing C. Chan,* Shi-Jian Ding,*‡ and Kai Fu*

From the Departments of Pathology and Microbiology and Environmental, Agricultural, and Occupational Health,† and the Mass Spectrometry and Proteomics Core Facility,‡ University of Nebraska Medical Center, Omaha, Nebraska*

The aberrant expression of microRNA-155 (miR-155), which has emerged as having a significant impact on the biological characteristics of lymphocytes, plays important roles in B-cell malignancies, such as diffuse large B-cell lymphoma (DLBCL). DLBCL is the most common non–Hodgkin's lymphoma in the adult population, accounting for approximately 40% of newly diagnosed non–Hodgkin's lymphoma cases globally. To determine the specific function of miR-155, a quantitative proteomics approach was applied to examine the inhibitory effects of miR-155 on protein synthesis in DLBCL cells. PIK3R1 (p85α), a negative regulator of the phosphatidylinositol 3-kinase (PI3K)–AKT pathway, was identified as a direct target of miR-155. A luciferase reporter was repressed through the direct interaction of miR-155 and the p85α 3′-untranslated region, and overexpression of miR-155 down-regulated both the transcription and translation of p85α. The PI3K-AKT signaling pathway was highly activated by the sustained overexpression of miR-155 in DHL16 cells, whereas knockdown of miR-155 in OCI-Ly3 cells diminished AKT activity. Taken together, our results reveal a novel target involved in miR-155 biological characteristics and provide a molecular link between the overexpression of miR-155 and the activation of PI3K-AKT in DLBCL. *(Am J Pathol 2012, 181:26–33; http://dx.doi.org/10.1016/j.ajpath.2012.03.013)*

MicroRNAs (miRNAs) are single-stranded RNAs of approximately 21 to 23 nucleotides that negatively regulate eukaryotic gene expression, mostly through base pairing with the 3′-untranslated region (UTR) of the target mRNA, leading to either inhibition of protein translation or increased mRNA degradation.[1,2] Among miRNAs expressed by hematopoietic cells, miR-155 has emerged as having a significant impact on the biological characteristics of lymphocytes.[3] Human miR-155 maps within and is processed from an exon of a noncoding RNA transcribed from the B-cell integration cluster (*BIC*) located on chromosome 21.[4] Normally, miR-155 is activated in response to B- or T-cell receptor engagement and plays an important role in germinal center formation and subsequent antibody production after antigen challenge.[5,6] However, beyond its apparent contribution to the humoral immune response, the need to properly regulate miR-155 levels is suggested by its dramatically elevated expression in several types of human B-cell lymphomas, such as primary mediastinal B-cell lymphoma, Burkitt's lymphoma, and diffuse large B-cell lymphoma (DLBCL).[7,8]

DLBCL is the most common non–Hodgkin's lymphoma in the adult population and accounts for approximately 40% of newly diagnosed non–Hodgkin's lymphoma cases worldwide.[9] It is a biologically and clinically heterogeneous disease, in part because of the diversity of its normal cell counterparts.[10,11] Gene expression profiling (GEP) has classified DLBCL into two main subcategories:

Supported by a scholarship from the China Scholarship Council (X.H.), a grant from the NIH (U01 CA114778-03 to W.C.C. and K.F.), a grant from the Nebraska Department of Health and Human Services (LB606 to S.-J.D.), and by a Lymphoma Research Foundation/Millennium Inc. Clinical Investigator Career Development Award (K.F.).

Accepted for publication March 22, 2012.

X.H. and Y.S. contributed equally to this work.

CME Disclosure: The authors of this article and the planning committee members and staff have no relevant financial relationships with commercial interest to disclose.

Supplemental material for this article can be found on http://ajp.amjpathol.org or at http://dx.doi.org/10.1016/j.ajpath.2012.03.013.

Address reprint requests to Kai Fu, M.D., Ph.D., Department of Pathology and Microbiology, 983135 Nebraska Medical Center, University of Nebraska Medical Center, Omaha, NE 68198-3135.. E-mail: kfu@unmc.edu.

germinal center B-cell-like (GCB) DLBCL and activated B-cell-like (ABC) DLBCL.[10,11] In general, ABC-DLBCL has a significantly poorer survival than GCB-DLBCL.[10,12] High miR-155 expression is more common in ABC-DLBCL.[13] However, the role of miR-155 overexpression in lymphomagenesis is largely unknown.

It is believed that miRNAs have the potential to regulate at least 20% to 30% of all human genes.[14] Recently, large-scale approaches for studying the regulatory effects of miRNAs have emerged, which include genome-wide computation of potential miRNA targets and experimental identification of miRNA-perturbed proteomic profiles.[15] The stable isotope labeling (SIL)–based quantitative proteomics technique, combined with liquid chromatography and tandem mass spectrometry (LC-MS/MS), has become the major approach for investigating comprehensive profiles of protein expression. Overexpressing an miRNA *in vitro* causes a mostly modest (usually lower than twofold) down-regulation of miRNA targets.[16] Although the proteins with decreased abundance are potential targets of miRNA, their abundance is influenced by additional factors, such as protein turnover. Thus, studies of the miRNA-perturbed profile of newly synthesized proteins, by pulsed SIL of amino acid in cell culture (pulsed SILAC), may provide better quantitation of targets and more effective miRNA target discovery.[16] In the current study, we used the pulsed SILAC technique to investigate the perturbation of protein synthesis by overexpression of miR-155 in DLBCL cells. Several targets of miR-155, such as WEE1, SHIP1, and PIK3R1 (p85α), were identified from the proteomics study. Functional studies indicated that the phosphatidylinositol 3-kinase (PI3K)–AKT pathway was constitutively activated by miR-155 overexpression in DLBCL.

Materials and Methods

DLBCL Cell Lines and Patient Samples

Four DLBCL cell lines, SU-DHL6, SU-DHL16 (hereafter, DHL16), OCI-Ly3, and OCI-Ly10, were used. SU-DHL6 and DHL16 are DLBCL lines with GCB GEP, whereas OCI-Ly3 and OCI-Ly10 are DLBCL lines with ABC GEP.[12,17] These cells were cultured in 90% RPMI 1640 medium with 10% fetal bovine serum, except that OCI-Ly3 used 90% Iscove's modified medium and OCI-Ly10 used 10% human serum.

Primary frozen tumor samples from 94 patients with *de novo* DLBCL who were treated with rituximab plus standard doxorubicin, cyclophosphamide, vincristine, and prednisone (CHOP) or CHOP-like therapy were retrieved from the Nebraska Lymphoma Study Group. The GEP information of 65 tumors was obtained by using the HG U133 Plus2 GeneChip following standard protocols (Affymetrix, Inc., Santa Clara, CA), as previously published (part of the Lymphoma/Leukemia Molecular Profiling Project consortium).[18] These patients were subclassified as having either the GCB or ABC type of DLBCL by their GEP information. Total RNA extracts from 67 of the patient tumor samples and four DLBCL lines were collected for miR-155 profiling. This study was approved by the Institutional Review Board of the University of Nebraska Medical Center, Omaha.

Construction of miR-155 Plasmid and Transfection

A *BIC* DNA fragment (669 bp) containing the miR-155 sequence was amplified from human genomic DNA. The primers used to clone miR-155 were as follows: forward, 5′-GATCAAAGTCTTCAAATATGCCTAAAGG-3′; and reverse, 5′-TGAACAAGCCAAAACCTGC-3′. The miR-155 DNA fragment was cloned downstream of green fluorescent protein (GFP) in an enhanced GFP (EGFP)–C2 vector, and the construct was confirmed by restrictive digestion and DNA sequencing. DHL16 cells were transiently transfected with this miR-155 expression construct (EGFP–miR-155) or control vector (EGFP-Ctrl) using the pmaxFP expression system (Amaxa, Gaithersburg, MD) with buffer V and program L29.[19] Transfection efficiency was evaluated by GFP expression and measured by real-time PCR.

SILAC Sample Preparation and SCX-NanoLC-MS/MS Analysis

Pulsed SILAC was used for quantitative proteomics analysis. For heavy labeling medium, L-[$^{13}C_6$]-lysine was used (Pierce Biotechnology, Rockford, IL); and for the light condition, L-[$^{12}C_6$]-lysine was used. DHL16 cells were cultured in normal RPMI 1640 medium, and transient transfection was performed. The cells were allowed to recover for 5 hours after transfection. Then, the cells transfected with miR-155 vector were cultured in the SILAC light medium, whereas the cells transfected with control vector were cultured in the SILAC heavy medium. Both cells were cultured in SILAC media for another 9 hours, and harvested separately in 8 mol/L urea lysis buffer. Then, based on their total protein abundances, equal masses of heavy and light lysates were mixed and tryptic digested, as previously described.[20]

Strong cation exchange (SCX) chromatography was performed on an Ultimate 3000 HPLC system (Dionex, Sunnyvale, CA), whereas the nanoLC-MS/MS analysis was performed using a NanoLC-2D LC system (Eksigent, Dublin, CA) and an linear ion trap (LTQ)-Orbitrap-XL mass spectrometer equipped with a nanospray ionization source (Thermo Scientific, San Jose, CA), as previously described.[20] Briefly, the mixture of tryptic peptides was separated by SCX into 20 fractions, and each fraction was analyzed by nanoLC-MS/MS. Survey full-scan MS spectra (from m/z 375 to 1575) were acquired in the Orbitrap with resolution $r = 100{,}000$. LTQ MS was operated in a data-dependent mode to automatically switch between the MS and MS/MS acquisitions. The most intense ions (top five) were sequentially isolated for fragmentation using collision-induced dissociation with a normalized collision energy of 30% and a target value of 5000.

Protein Identification and Quantification

MS raw data were deisotoped and converted to the mgf files,[20] then submitted to the Mascot (Matrix Science, London, UK) search engine for peptide identification against the human international protein index database (version 3.52) with the decoy database technique. Carbamidomethylation of cysteine was used as a fixed modification, and oxidation of methionine was used as a variable modification. The initial mass deviation tolerance of precursor ion was set to 20 ppm, and the fragment ion tolerance was set to 0.5 Da. A maximum of two missed cleavages was allowed in peptide identification.

After the database search, the resulting dat files and MS raw data were imported into the UNiquant software for protein quantitation.[20] All spectra of identified peptides with a Mascot score >10 were quantified to obtained the intensities of the heavy and light counterpart. A cutoff of signal/noise ratio higher than two was applied to remove the low-confidence peaks. Then, a criterion, termed quality of peptide identification,[20] based on the Mascot score and mass accuracy of the precursor, was used to filter the quantified peptides and proteins, respectively, using a false discovery rate <0.01. Finally, locally weighted scatterplot smoothing (Lowess) method[21] was used to normalize the heavy/light ratios of quantified proteins, using the sum of intensities for the heavy species divided by the light species for each protein.

Knockdown of p85α by siRNA

Small-interfering RNAs (siRNAs) that specifically inhibit p85α (ON-TARGETplus SMARTpoll siRNA and ON-TARGETplus Non-targeting pool) were obtained from Dharmacon Inc. (Chicago, IL). One million DHL16 cells were transfected with either 0.2 nmol/L p85α siRNA or control siRNA using the pmaxFP expression system. Cells were harvested 24 hours after treatment.

Transduction of DHL16 and OCI-Ly3 Cells

The tetracycline-regulated retroviral vector TMP (OpenBioSystem, Huntsville, AL) was modified by deleting miR-30 sequences. The miR-155 sequence was cloned into this retrovirus vector (with Tet-On regulation system), following a protocol as previously described.[22] This retrovirus vector was named pTIP-miR-155 and transduced into DHL16 cells to establish a B-cell line with sustained expression of miR-155. The pTIP-GFP vector (without miR-155) was transduced into DHL16 cells as a negative control.

Construction of the pTIP-miR-155-sponge vector follows the protocol described by Sharp and coworkers.[23] The microRNA sponge plasmid and the control vector were initially obtained from the laboratory of Sharp and coworkers, and modified to competitively inhibit miR-155. Briefly, oligonucleotides containing miR-155 binding sites with four-nucleotide spacers to provide a central bulge were annealed, self-ligated, gel purified, and cloned into pcDNA5-CMV-d2eGFP vector (Invitrogen, Carlsbad, CA). Subclones containing 11 tandem copies of the sponge sites were identified and confirmed by sequencing, and then inserted into the pTIP-GFP vector (downstream of GFP). OCI-Ly3 cells were transduced with the pTIP-miR-155-sponge vector to establish a B-cell line with sustained inhibition of miR-155. All transduced cells were positively selected by puromycin for 2 weeks and evaluated for GFP expression.

RT-qPCR

For quantitative RT-PCR (RT-qPCR), miR-155 expression was measured by the real-time qPCR-based TaqMan human microRNA assay from Applied Biosystems (Foster City, CA), according to the standard protocol. RNA was isolated using the mirVana miRNA Isolation Kit (Ambion, Austin, TX) and reverse transcribed with both miR-155 and U6 primers. The data set was normalized using the average expression of U6 small-nuclear RNA.

To evaluate mRNA expression, total RNA was extracted using TRIzol reagent, and 1 μg of total RNA from patient samples was used for RT (Invitrogen). Primers used were as follows: p85α, 5′-GCTGAGAAAGACGAGAGACC-3′ (forward) and 5′-TTCATCATCTTCCACCAGTG-3′ (reverse); and glyceraldehyde-3-phosphate dehydrogenase, 5′-CGACCACTTTGTCAAGCTCA-3′ (forward) and 5′-CCCTGTTGCTGTAGCCAAAT-3′ (reverse). Two replicates were included for each measurement.

Luciferase Activity Assay

Sequences of the 3′-UTR of human p85α gene (human PIK3R1, NM_181504) were cloned with the following primers: forward, 5′-GTCCTACTGATGTTCCTTTGG-3′; reverse, 5′-AACTGACCGTGACATCCTC-3′; and mutation, 5′-GTCACCATGAGAT*AGATCTA*GCTGCCCAGGATG-3′ (mutated sites italicized). The DNA insert was introduced downstream of the luciferase reporter gene in the pGL3 promoter vector (Promega, Madison, WI). Luciferase activity assays were performed with the Dual-Luciferase Reporter System (Promega). HEK-293T cells were cotransfected with luciferase reporter plasmids (250 ng) and miR-155 expression vector (750 ng). Luciferase activities were measured 48 hours after transfection.

Cell Viability Assay

Transduced DHL16 and OCI-Ly3 cells were plated at a density of 10,000 cells per well into a six-well plate. Cell proliferation was examined at 0, 1, 2, 4, and 6 days after seeding. Doxycycline (1 μg/mL) was added every other day. Culture medium, 100 μL, was added together with 20 μL of Cell Titer 96AQueousOne solution (Promega) and then incubated at 37°C for 2 hours (three replicates). Optical density was measured at 490 nm using a plate reader.

Western Blot Analysis

Preparation of cell lysates and Western blot analysis were performed as previously described.[19] Primary antibodies included the following: p85α (Genscript, Piscataway, NJ),

β-actin, phosphatidylinositol-3,4,5-trisphosphate 5-phosphatase 1 (SHIP1; Santa Cruz Biotechnology, Santa Cruz, CA), phosphorylated glycogen synthetase kinase 3β (Ser9; Signalway Antibody, Pearland, TX), phosphorylated AKT (Ser473), phosphorylated AKT (Thr308), and AKT (Cell Signaling, Danvers, MA).

Results

Expression of BIC Transcripts and miR-155 in Patients with DLBCL

We examined the expression levels of *BIC*, the miR-155 precursor transcript, in patients with DLBLC. The average *BIC* expression in 41 patients with GCB-DLBCL and 24 patients with ABC-DLBCL was calculated from GEP data. As shown in Figure 1A, the ABC subgroup cases had a significantly higher (P = 6.24E-07) expression of *BIC* transcripts than the GCB subgroup.

Next, we studied the basal expression of mature miR-155 by RT-qPCR in two GCB-DLBCL lines (SU-DHL6 and DHL16), two ABC-DLBCL cells (OCI-Ly3 and OCI-Ly10), and the frozen tumor samples of 36 patients with GCB-DLBCL and 31 patients with ABC-DLBCL. The ABC subgroup of cases had a significantly higher (P = 6.86E-05) expression of mature miR-155 than the GCB subgroup (Figure 1B). Two GCB-DLBCL lines (SU-DHL6 and DHL16) had lower expression of miR-155 compared with the two ABC-DLBCL lines (OCI-Ly3 and OCI-Ly10). Our data indicated that the ABC-DLBCL subgroup was significantly more likely to overexpress miR-155 compared with the GCB-DLBCL subgroup.

Quantitative Proteomics Reveals Potential Targets of miR-155

Because DHL16 cells had a relatively low expression of miR-155, we overexpressed miR-155 in DHL16 cells by transient transfection. RT-qPCR indicated that approximately 1000-fold overexpression of miR-155 was obtained in cells with EGFP-miR-155 transfection compared with the EGFP-Ctrl group (see Supplemental Figure S1 at *http://ajp.amjpathol.org*). LC-MS/MS–based quantitative proteomics with pulsed SILAC labeling was performed to study the impact of miR-155 overexpression on protein output. As illustrated in Figure 2A, newly synthesized proteins were labeled for 9 hours by SILAC heavy medium, beginning 5 hours after transfection in the EGFP-Ctrl cells. Cells in the EGFP–miR-155 groups were similarly kept in SILAC light medium for 9 hours.

Equal masses of heavy and light cell lysates were mixed, digested, and analyzed by LC-MS/MS. By using Mascot for peptide identification and UNiquant for peptide and protein quantification,[20] a total of 2103 proteins were quantified from 6569 unique peptides, with a false-

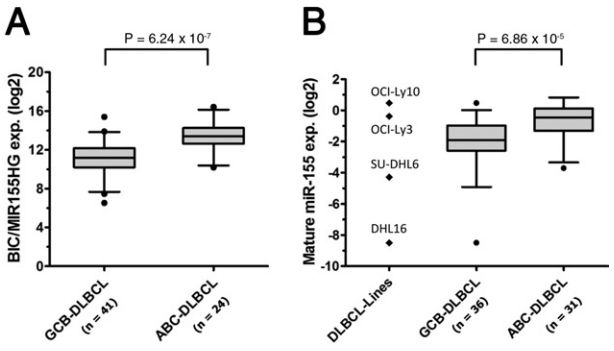

Figure 1. miR-155 expression (exp.) in patients with DLBCL and cell lines. **A:** Expression of *BIC/MIR155HG* transcripts in patients with ABC-DLBCL (n = 24) and GCB-DLBCL (n = 42). Expression based on GEP analysis is shown in a box-and-whiskers plot (5th and 95th percentiles). **B:** Expression of mature miR-155 detected by RT-qPCR in four DLBLC cell lines (OCI-Ly3, OCI-Ly10, SU-DHL6, and DHL16), patients with ABC-DLBCL (n = 31), and patients with GCB-DLBCL (n = 30). All miR-155 expression data are normalized to the endogenous U6 RNA expression level by the following formula: $\Delta C_T = C_T(U6) - C_T(miR\text{-}155)$. GraphPad Prism software version 5.0 (La Jolla, CA) is used to analyze and visualize the expression data.

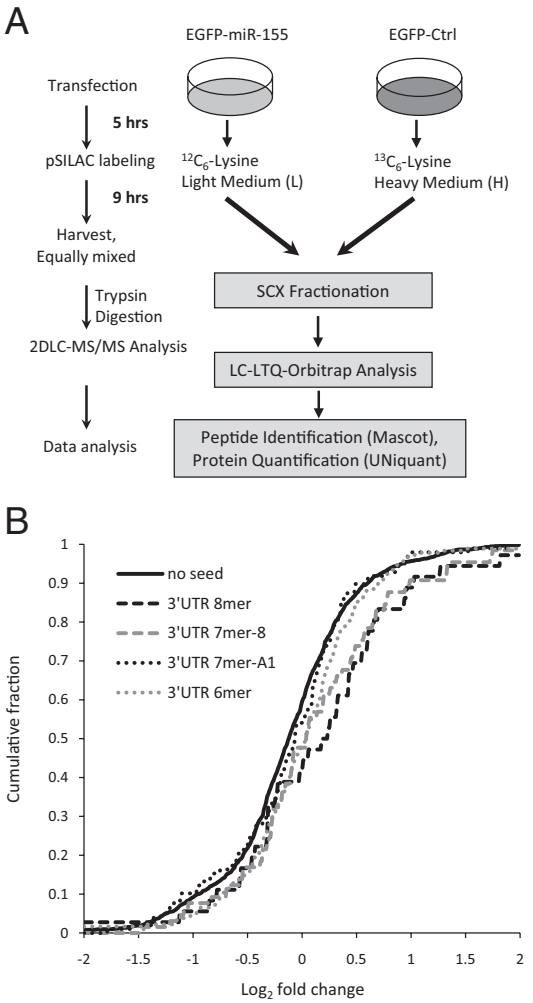

Figure 2. Quantitative proteomics for discovering miR-155 targets. **A:** Work flow of the proteomics strategy with pulsed SILAC labeling. DHL16 cells are transiently transfected with either EGFP-miR-155 or EGFP-Ctrl plasmid. Culture medium is changed 5 hours after transfection, and cells are harvested 9 hours later. Then, the cell lysates are mixed at equal protein masses and subjected to tryptic digestion, SCX fractionation, and LC-LTQ-Orbitrap analysis. Peptides are identified by Mascot, and proteins are quantified by UNiquant. **B:** Response of protein synthesis to altered miR-155. Cumulative distributions of different seed classes for the quantified proteins are plotted. Matches of miR-155 and 3′-UTR of mRNA are as follows: positions 1-8 (3′-UTR 8mer), 2–8 (3′-UTR 7mer-8), 2–7 with adenosine in position 1 (3′-UTR 7mer-A1), and 2–7 (3′-UTR 6mer).

discovery rate of <0.01 (see Supplemental Table S1 at *http://ajp.amjpathol.org*). We used the Lowess method[24] to normalize the quantified ratios of proteins, by assuming that the rate of synthesis of most proteins was not changed by miR-155 treatment (see Supplemental Figure S2A at *http://ajp.amjpathol.org*). After Lowess normalization, heavy/light (H/L) ratios of quantified proteins followed a gaussian-like distribution (see Supplemental Figure S2B at *http://ajp.amjpathol.org*). In our proteomics study, proteins with high H/L ratios were the proteins whose synthesis was repressed by miR-155 overexpression. Because miRNAs may target mRNAs primarily by binding to seed sequences in the 3′-UTRs, we searched the National Center for Biotechnology Information RefSeq database of human transcripts to identify the 3′-UTR sequence motifs that miR-155 can potentially target. Different seed classes for miR-155 were generated by matching to positions 1–8 (3′-UTR 8mer), 2–8 (3′-UTR 7mer-m8), 2–7 with adenosine in position 1 (3′-UTR 7mer-1A), and 2–7 (3′-UTR 6mer), according to the algorithm of TargetScan.[25] Of the proteins containing 3′-UTR 8mer or 3′-UTR 7mer-m8 seeds, 21 were up-regulated by >1.25-fold (H/L <0.8), whereas 34 were inhibited by >1.25-fold (H/L >1.25). For proteins without miR-155 seeds, 453 were up-regulated, whereas 259 were down-regulated, by >1.25-fold. Proteins with miR-155 seeds were significantly enriched in the down-regulated proteins after miR-155 transfection (Fisher's exact test, $P = 0.0003$). The cumulative frequency curves for the 3′-UTR 8mer and 3′-UTR 7mer-m8 groups showed a rightward shift compared with the other groups in the right part of Figure 2B, indicating that the effect of miR-155 on the cumulative curves was mainly through the inhibition of the proteins, with down-regulation by miR-155 transfection.

Conservation of the miR-155 binding sequence was another important factor in predicting the repressive effect on miR-155 targets.[25] Ten proteins (WEE1, FXR1, PEA15, GATAD2B, CAB39, PIK3R1, DNAJB1, CHAFIA, INPP5D, and LSM14A) showed both conserved seed sequences in their 3′-UTR and repressed protein production (see Supplemental Table S2 at *http://ajp.amjpathol.org*). All these proteins contained the 3′-UTR 8mer or 3′-UTR 7mer-m8 type of miR-155 seed, which were the two most stable seed sequences. WEE1 (WEE1 homolog–*Schizosaccharomyces pombe*), a cell-cycle regulator, was quantified, with an H/L ratio of 3.52. It was previously reported that overexpression of miR-155 enhanced the mutation rate and decreased the efficiency of DNA checkpoint mechanisms by targeting WEE1 in inflammation and cancers.[26] Quantitative proteomics also identified two negative regulators of the PI3K-AKT pathway, INPP5D (SHIP1) and PIK3R1 (P85α), both of which were down-regulated by miR-155 and contained conserved binding sites for miR-155 (see Supplemental Table S2 at *http://ajp.amjpathol.org*). MS-based identification and quantification of these two proteins are illustrated in Supplemental Figure S3 (available at *http://ajp.amjpathol.org*). SHIP1 was identified as a direct target of miR-155 in previous studies.[27] P85α, a novel target of miR-155, was a regulatory subunit of PI3K, with dual activation and repressive roles. Binding of p85α by activated receptor tyrosine kinases or adaptor proteins relieved the basal repression of p110, the catalytic subunit of PI3K, leading to the activation of AKT.[28]

P85α Is a Direct Target of miR-155

The 3′-UTR of p85α contained a predicted binding site for miR-155, which was conserved among several species, including human, mouse, rabbit, and dog (Figure 3A). To

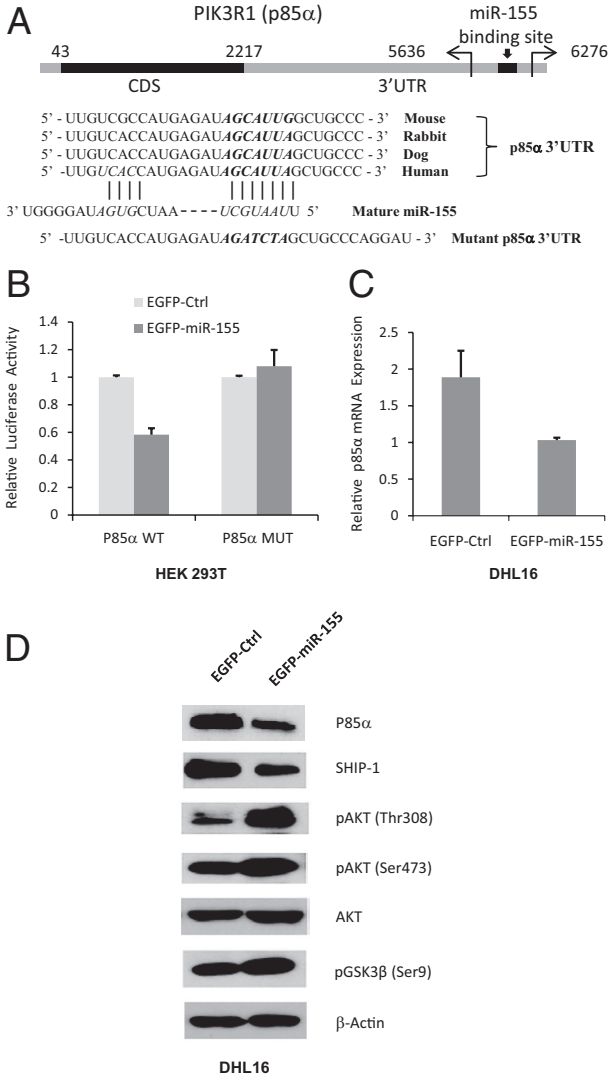

Figure 3. miR-155 activates the PI3K-AKT signaling pathway by targeting p85α. **A:** Schematic layout of the p85α mRNA (NM_181504). The predicted miR-155 binding site is indicated. This binding site is conserved within the p85α 3′-UTR from different species. A fragment of the p85α 3′-UTR (nucleotides 5636 to 6276, which contain the miR-155 seed site) is cloned to downstream of luciferase report vector, and a construct containing a mutation in the seed sequence is also generated. **B:** Luciferase reporter constructs containing the 3′-UTR of WT p85α or with point mutations (MUTs) in the miR-155 binding site are cotransfected with either EGFP-miR-155 or EGFP-Ctrl vectors in HEK-293T cells. Data are shown as mean ± SD of luciferase activity (three replicates). **C:** Relative expressions of p85α mRNA in DHL16 cells transfected with either EGFP-miR-155 or EGFP-Ctrl. **D:** The PI3K-AKT signaling pathway is activated by miR-155 in DHL16 cells. P85α and SHIP1 are repressed, and phosphorylation of AKT (pAKT; Ser473 and Thr308) and glycogen synthetase kinase (GSK) 3β (Ser9) is increased by miR-155 activation.

directly test whether p85α can be repressed by direct interaction with its 3′-UTR, we cloned its 3′-UTR into a luciferase reporter plasmid. This reporter vector was cotransfected with either EGFP-C2-miR-155 or EGFP-C2 vector into HEK-293T cells. We observed an approximately 40% decrease in luciferase activity when 293T cells were cotransfected with EGFP-miR-155 vector and luciferase-p85α wild-type (WT) 3′-UTR, compared with the cells cotransfected with EGFP-Ctrl vector. However, cotransfection of EGFP-miR-155 failed to repress the luciferase activity if the p85α 3′-UTR contained a mutated miR-155 seed sequence (Figure 3B). Furthermore, overexpression of miR-155 repressed p85α mRNA expression by approximately 50% (Figure 3C) and also repressed p85α protein expression (Figure 3D). By targeting SHIP1 and p85α, the PI3K-AKT pathway was activated in DHL16 cells with miR-155 overexpression. Western blot analysis indicated that expression of phosphorylated AKT (Ser473 and Thr308) was increased by miR-155 overexpression. Glycogen synthetase kinase 3β, a downstream effecter protein after AKT activation, also showed increased phosphorylation at Ser9 (Figure 3D).

Overexpression of miR-155 Activates the PI3K-AKT Pathway in DLBCL

To determine whether miR-155 can activate the PI3K-AKT pathway through repressing endogenous p85α, we introduced p85α-specific siRNA to knock down the expression of p85α. As shown in Figure 4A, DHL16 cells transfected with anti-p85α siRNA showed decreased expression of p85α. Down-regulation of p85α increased AKT phosphorylation compared with DHL16 cells transfected with control siRNA.

Retroviral vectors containing either the miR-155 construct sequence or the miR-155–specific sponge sequence within the 3′-UTR of GFP were used to transduce DLBCL cells with sustained overexpression or inhibition of miR-155, respectively (Figure 4B). DHL16, which is a GCB-DLBCL cell line with low expression of miR-155, was transduced with pTIP-miR-155 vectors. Ectopic overexpression of miR-155 up-regulated AKT activity, presumably by directly targeting p85α (Figure 4B). Next, we transduced the pTIP-miR-155-sponge retrovirus into OCI-Ly3 cells, which is an ABC-DLBCL cell line with high expression of miR-155. Knockdown of miR-155 down-regulated AKT activity, presumably at least partially by releasing the repressing effect on p85α (Figure 4B).

Because the effects of AKT activation include increased cell proliferation and inhibition of apoptosis, we studied cell viability in DHL16 cells with or without sustained overexpression of miR-155. As shown in Figure 4C, DHL16 cells transduced with pTIP-miR-155 have increased cell viability at 4 days. At day 6, the pTIP-miR-155 group had significantly higher ($P < 0.05$) viability compared with the pTIP-GFP and WT groups. The cell viability of OCI-Ly3 cells transduced with the pTIP-miR-155-sponge was also examined. OCI-Ly3 cells with sustained inhibition of miR-155 exhibited lower ($P < 0.05$) cell viability compared with the other two groups of cells (Figure 4D).

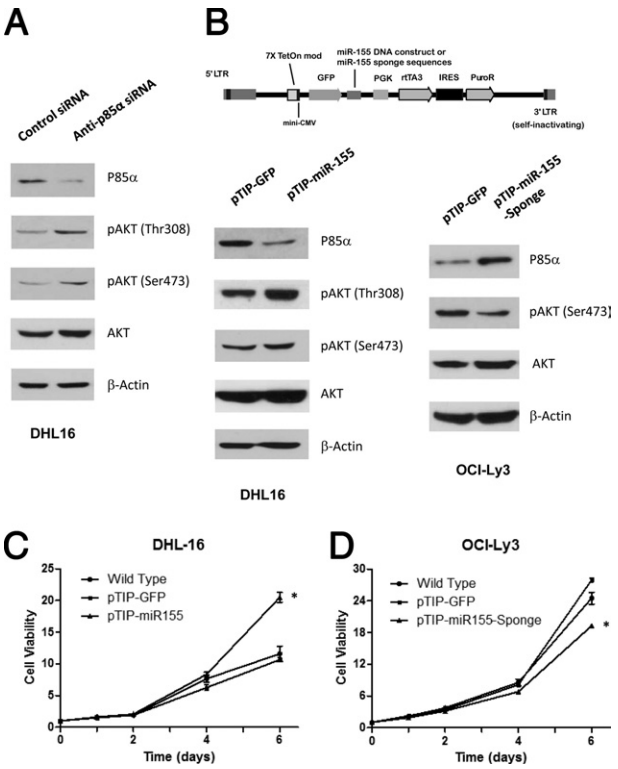

Figure 4. Constitutively overexpressing miR-155 activates PI3K-AKT signaling and increases cell viability. **A:** Knockdown of p85α by siRNA decreases the phosphorylation (Ser473 and Thr308) of AKT in DHL16 cells. **B:** Use of the retroviral vector with a Tet-On regulation system (pTIP-GFP). Either miR-155 DNA constructs (pTIP-miR-155) or an miR-155 sponge sequence with 11 tandem repeats of the miR-155 binding site (pTIP-miR-155-sponge) is cloned downstream of GFP. Transduction of DHL16 cells with pTIP-miR-155 increases AKT phosphorylation (pAKT; Ser473 and Thr308), and transduction of OCI-Ly3 cells with pTIP-miR-155-sponge decreases phosphorylation (Ser473) of AKT. **C:** Cell viability of WT DHL16 cells or cells transduced with pTIP-GFP or pTIP-miR1-155 vectors. *$P < 0.05$ compared with untransduced or pTIP-GFP–transduced cells. **D:** Cell viability of untransduced OCI-Ly3 cells or cells transduced with pTIP-GFP or pTIP-miR1-155-sponge vectors. *$P < 0.05$ compared with untransduced or pTIP-GFP–transduced cells. Data are shown as mean ± SD (three replicates).

Discussion

miR-155 has emerged as an important regulator with impact on tumorigenesis of several types of human lymphomas. Our data revealed that patients with ABC-DLBCL have significantly higher expression of miR-155 compared with the GCB subtype. By using the pulsed SILAC technique, we determined that several key regulators, such as WEE1, SHIP1, and p85α, were regulated by miR-155. Functional analysis indicated that AKT activity in DLBCL was regulated by miR-155 through direct targeting of p85α, a positive and negative regulator of the PI3K-AKT pathway. Although p85α stabilizes p110 and recruits it to activated surface receptors, it inhibits its activity in the absence of stimulation. In addition, in many cell types, p85α is in stoichiometric excess, and the free subunit can compete with the p85α-p110 heterodimer for receptor binding.[29]

A recent clinical study[30] showed that activity of the PI3K-AKT pathway is a prognostic marker in DLBCL. The oncogenic effects of AKT in DLBCL are numerous, including, among others, activation of mammalian target of rapamycin signaling[31]; increased glucose metabolism, which promotes MCL1 synthesis and resistance to BCL2 inhibition[32]; and inhibition of apoptosis through expression of XIAP.[33] GEP analysis of DLBCL indicated that ABC-DLBCLs generally exhibit high NF-κB activity, whereas GCB-DLBCLs express high levels of proliferation- and metabolism-related genes.[12] AKT activity is essential for survival of some, but not all, DLBCL cell lines of both subtypes, but it may be regulated differently in the two. In the ABC subtype, NF-κB activation plays an important role for tumor survival[34]; part of its effect may be through the induction of miR-155 in this subtype, contributing to constitutive AKT activity and inhibition of cell death.

Aberrant overexpression of miRNAs activates PI3K-AKT signaling by down-regulation of its suppressors (eg, repressing PTEN by miR-21 and miR-17-92).[35] SHIP1, another negative regulator of the PI3K-AKT pathway, was previously identified as a direct target of miR-155.[27] PI3K and PTEN antagonistically control signaling from phosphatidylinositol (3,4,5)-trisphosphate (PIP3) to AKT phosphorylation and activation. A role of PTEN and PI3K in tumorigenesis is supported by the observation that somatic mutations of these proteins occur frequently and result in constitutive activation of AKT in human cancers.[36] Our data indicated that p85α, the PI3K regulatory subunit, was directly repressed by miR-155. Overexpression of miR-155 activates the PI3K-AKT signaling pathway, which is likely, at least in part, through down-regulation of p85α. Furthermore, our data demonstrated that gain of function for miR-155 in a GCB cell line with low miR-155 expression activates AKT and, hence, increases cell viability, whereas, conversely, down-regulation of miR-155 diminishes AKT activity and decreases cell viability in an ABC cell line with high expression of miR-155. Moreover, normal function of PTEN requires p85α binding at its N-terminal SH3 domain to enhance PTEN lipid phosphatase activity.[28,29] Considering the central role of PTEN activity in regulating AKT phosphorylation, inhibition of p85α by miR-155 may have dual functions: abrogating p110-inhibitory activity and preventing the recruitment of PTEN, both resulting in the enhancement of AKT signaling.

In summary, our study revealed a novel molecular mechanism by which miR-155, through direct targeting and repressing p85α, activates oncogenetic AKT signaling in DLBCL.

Acknowledgment

We thank Dr. Phillip A. Sharp for providing the sponge plasmids.

References

1. Lee RC, Ambros V: An extensive class of small RNAs in Caenorhabditis elegans. Science 2001, 294:862–864
2. Bartel DP: MicroRNAs: genomics, biogenesis, mechanism, and function. Cell 2004, 116:281–297
3. Ramkissoon SH, Mainwaring LA, Ogasawara Y, Keyvanfar K, McCoy JP Jr, Sloand EM, Kajigaya S, Young NS: Hematopoietic-specific microRNA expression in human cells. Leuk Res 2006, 30:643–647
4. Lagos-Quintana M, Rauhut R, Yalcin A, Meyer J, Lendeckel W, Tuschl T: Identification of tissue-specific microRNAs from mouse. Curr Biol 2002, 12:735–739
5. Turner M, Vigorito E: Regulation of B- and T-cell differentiation by a single microRNA. Biochem Soc Trans 2008, 36:531–533
6. Ademokun A, Turner M: Regulation of B-cell differentiation by microRNAs and RNA-binding proteins. Biochem Soc Trans 2008, 36:1191–1193
7. Metzler M, Wilda M, Busch K, Viehmann S, Borkhardt A: High expression of precursor microRNA-155/BIC RNA in children with Burkitt lymphoma. Genes Chromosomes Cancer 2004, 39:167–169
8. Kluiver J, Poppema S, de Jong D, Blokzijl T, Harms G, Jacobs S, Kroesen BJ, van den Berg A: BIC and miR-155 are highly expressed in Hodgkin, primary mediastinal and diffuse large B cell lymphomas. J Pathol 2005, 207:243–249
9. World Health Organization: WHO Classification of Tumours of Haematopoietic and Lymphoid Tissues. Geneva, Switzerland, WHO Press, 2008
10. Rosenwald A, Wright G, Chan WC, Connors JM, Campo E, Fisher RI, et al: The use of molecular profiling to predict survival after chemotherapy for diffuse large-B-cell lymphoma. N Engl J Med 2002, 346:1937–1947
11. Wilson WH, Dunleavy K, Pittaluga S, Hegde U, Grant N, Steinberg SM, Raffeld M, Gutierrez M, Chabner BA, Staudt L, Jaffe ES, Janik JE: Phase II study of dose-adjusted EPOCH and rituximab in untreated diffuse large B-cell lymphoma with analysis of germinal center and post-germinal center biomarkers. J Clin Oncol 2008, 26:2717–2724
12. Alizadeh AA, Eisen MB, Davis RE, Ma C, Lossos IS, Rosenwald A, Boldrick JC, Sabet H, Tran T, Yu X, Powell JI, Yang L, Marti GE, Moore T, Hudson J Jr, Lu L, Lewis DB, Tibshirani R, Sherlock G, Chan WC, Greiner TC, Weisenburger DD, Armitage JO, Warnke R, Levy R, Wilson W, Grever MR, Byrd JC, Botstein D, Brown PO, Staudt LM: Distinct types of diffuse large B-cell lymphoma identified by gene expression profiling. Nature 2000, 403:503–511
13. Lawrie CH, Soneji S, Marafioti T, Cooper CD, Palazzo S, Paterson JC, Cattan H, Enver T, Mager R, Boultwood J, Wainscoat JS, Hatton CS: MicroRNA expression distinguishes between germinal center B cell-like and activated B cell-like subtypes of diffuse large B cell lymphoma. Int J Cancer 2007, 121:1156–1161
14. Lim LP, Lau NC, Garrett-Engele P, Grimson A, Schelter JM, Castle J, Bartel DP, Linsley PS, Johnson JM: Microarray analysis shows that some microRNAs downregulate large numbers of target mRNAs. Nature 2005, 433:769–773
15. Baek D, Villen J, Shin C, Camargo FD, Gygi SP, Bartel DP: The impact of microRNAs on protein output. Nature 2008, 455:64–71
16. Selbach M, Schwanhausser B, Thierfelder N, Fang Z, Khanin R, Rajewsky N: Widespread changes in protein synthesis induced by microRNAs. Nature 2008, 455:58–63
17. Ramachandrareddy H, Bouska A, Shen Y, Ji M, Rizzino A, Chan WC, McKeithan TW: BCL6 promoter interacts with far upstream sequences with greatly enhanced activating histone modifications in germinal center B cells. Proc Natl Acad Sci U S A 2010, 107:11930–11935
18. Lenz G, Wright G, Dave SS, Xiao W, Powell J, Zhao H, et al: Stromal gene signatures in large-B-cell lymphomas. N Engl J Med 2008, 359:2313–2323
19. Shen Y, Ge B, Ramachandrareddy H, McKeithan T, Chan WC: Alternative splicing generates a short BCL6 (BCL6S) isoform encoding a compact repressor. Biochem Biophys Res Commun 2008, 375:190–193
20. Huang X, Tolmachev AV, Shen Y, Liu M, Huang L, Zhang Z, Anderson GA, Smith RD, Chan WC, Hinrichs SH, Fu K, Ding SJ: UNiquant, a program for quantitative proteomics analysis using stable isotope labeling. J Proteome Res 2011, 10:1228–1237

21. Cleveland WS: Robust locally weighted regression and smoothing scatterplots. J Am Stat Assoc 1979, 74:829–836
22. Rao E, Jiang C, Ji M, Huang X, Iqbal J, Lenz G, Wright G, Staudt LM, Zhao Y, McKeithan TW, Chan WC, Fu K: The miRNA-17~92 cluster mediates chemoresistance and enhances tumor growth in mantle cell lymphoma via PI3K/AKT pathway activation. Leukemia 2012, 26: 1064–1072
23. Ebert MS, Neilson JR, Sharp PA: MicroRNA sponges: competitive inhibitors of small RNAs in mammalian cells. Nat Methods 2007, 4:721–726
24. Smyth GK, Speed T: Normalization of cDNA microarray data. Methods 2003, 31:265–273
25. Lewis BP, Burge CB, Bartel DP: Conserved seed pairing, often flanked by adenosines, indicates that thousands of human genes are microRNA targets. Cell 2005, 120:15–20
26. Tili E, Michaille JJ, Wernicke D, Alder H, Costinean S, Volinia S, Croce CM: Mutator activity induced by microRNA-155 (miR-155) links inflammation and cancer. Proc Natl Acad Sci U S A 2011, 108:4908–4913
27. O'Connell RM, Chaudhuri AA, Rao DS, Baltimore D: Inositol phosphatase SHIP1 is a primary target of miR-155. Proc Natl Acad Sci U S A 2009, 106:7113–7118
28. Engelman JA: Targeting PI3K signalling in cancer: opportunities, challenges and limitations. Nat Rev Cancer 2009, 9:550–562
29. Chagpar RB, Links PH, Pastor MC, Furber LA, Hawrysh AD, Chamberlain MD, Anderson DH: Direct positive regulation of PTEN by the p85 subunit of phosphatidylinositol 3-kinase. Proc Natl Acad Sci U S A 2010, 107:5471–5476
30. Uddin S, Hussain AR, Siraj AK, Manogaran PS, Al-Jomah NA, Moorji A, Atizado V, Al-Dayel F, Belgaumi A, El-Solh H, Ezzat A, Bavi P, Al-Kuraya KS: Role of phosphatidylinositol 3′-kinase/AKT pathway in diffuse large B-cell lymphoma survival. Blood 2006, 108:4178–4186
31. Wanner K, Hipp S, Oelsner M, Ringshausen I, Bogner C, Peschel C, Decker T: Mammalian target of rapamycin inhibition induces cell cycle arrest in diffuse large B cell lymphoma (DLBCL) cells and sensitises DLBCL cells to rituximab. Br J Haematol 2006, 134:475–484
32. Coloff JL, Macintyre AN, Nichols AG, Liu T, Gallo CA, Plas DR, Rathmell JC: Akt-dependent glucose metabolism promotes Mcl-1 synthesis to maintain cell survival and resistance to Bcl-2 inhibition. Cancer Res 2011, 71:5204–5213
33. Hussain AR, Uddin S, Ahmed M, Bu R, Ahmed SO, Abubaker J, Sultana M, Ajarim D, Al-Dayel F, Bavi PP, Al-Kuraya KS: Prognostic significance of XIAP expression in DLBCL and effect of its inhibition on AKT signalling. J Pathol 2010, 222:180–190
34. Lenz G, Davis RE, Ngo VN, Lam L, George TC, Wright GW, Dave SS, Zhao H, Xu W, Rosenwald A, Ott G, Muller-Hermelink HK, Gascoyne RD, Connors JM, Rimsza LM, Campo E, Jaffe ES, Delabie J, Smeland EB, Fisher RI, Chan WC, Staudt LM: Oncogenic CARD11 mutations in human diffuse large B cell lymphoma. Science 2008, 319:1676–1679
35. Wang Y, Lee CG: MicroRNA and cancer: focus on apoptosis. J Cell Mol Med 2009, 13:12–23
36. Abubaker J, Bavi PP, Al-Harbi S, Siraj AK, Al-Dayel F, Uddin S, Al-Kuraya K: PIK3CA mutations are mutually exclusive with PTEN loss in diffuse large B-cell lymphoma. Leukemia 2007, 21:2368–2370